

Analysis of Concrete Beams During the Corrosion Process on Reinforcement Under Tensile Stress

N. F. Ortega* and R. R. Aveldaño

Departamento de Ingeniería, Universidad Nacional del Sur, Bahía Blanca, Argentina

Abstract: This paper aims to the experimental study of reinforced concrete beams subjected to mechanical stresses and simultaneously affected by a corrosion process of their reinforcements. The corrosion process is galvanostatically accelerated applying a certain current density to a limited area of the reinforcements, which are under constant wetting with a solution of Sodium Chloride. The influence of the different degrees of tension in the process of reinforcement corrosion is analyzed through electrochemical monitoring, the cracking advancement in the concrete cover, and the loss of base material in the bars.

Key Words: Reinforced concrete, stress corrosion, cracking.

INTRODUCTION

It is very well known that concrete's resistance to tensile stress is low, a fact that leads to the introduction of steel bars inside its mass, so that these bars absorb the tensile stresses. In this way, both reinforced and pre-stressed concrete overcome the usage limitations of plain concrete.

In standard conditions (in non-aggressive environments, under careful elaboration, working and execution), concrete provides enough protection to the steel bars against corrosion due to its alkalinity, for a certain period of time. But if any of those conditions is not met, corrosion problems could begin in the reinforcement bars (rebars), which could lead to the element's or structure's collapse.

Previous papers deal with the corrosion problem under different conditions. In some cases [1-5], reinforced concrete beams are subjected only to their own weight, without external load; rebars are totally in tension while concrete is partially in tension and compression.

In other papers [6, 7], pre-stressed concrete beams are analyzed; in these cases, active steel bars are also totally in tension while concrete is totally compressed having no tension stresses.

In this paper, in order to simulate as accurately as possible the real conditions of reinforced concrete structures, it was analyzed the behavior of reinforced concrete beams under variable external loads, when an accelerated corrosion process is applied simultaneously. Several analysis methods were used, to assess the influence of tension increase on the rebars on corrosive state, as manifestation of different effects, some external and some internal.

MATERIALS AND METHODOLOGY

Beams Construction

In the construction of the beams an attempt was made to reproduce, as accurately as possible, similar conditions to the

ones that commonly present in practice. Therefore, the dimensions of the reinforced concrete beams were chosen so as to keep a geometric equivalence with those used in real construction sites (approximate scale 1:3): 2.20 m length, 0.08 x 0.16 m cross-section, longitudinal reinforcements constituted by four 4.2 mm nominal diameter steel bars (two on the top and two on the bottom of the beam) and closed stirrups made of 2.1 mm nominal diameter wire, spaced every 0.10 m.

Concrete was poured inside the moulds, then vibrated mechanically in three layers and cured during the first 7 days. Until the time of the test (which took place around a year after the construction of the samples), the beams were kept in laboratory environment (temperature around 20 °C, relative humidity around 50 %). Cylindrical test samples (0.15 x 0.30 m) were also made and then tested, in order to determine their tensile and compressive strength, in accordance with IRAM Standard 1546 [8] and ASTM-C496-71 Standard [9] respectively.

Employed Materials

Characteristics of the steel used in the beams, are shown in Table 1, and those ones of the employed concrete are shown in Table 2.

It must be pointed out that the water/cement ratio adopted along the tests does not coincide with that one of the most of recent standards (in Argentina, $w/c \leq 0.5$ indicates by CIR-SOC 201 [12]). In order to increase porosity to enhance the corrosion effects, a ratio $w/c=0.58$ has been adopted for the beams instead of the standard values. It would favour the observation into a period of five months of the research. On the other hand, it must bear in mind that frequently it can be find concrete structures into chlorides environments which are affected by corrosion out of that standard.

Process of Corrosion Under Stress

In order to apply tensile stresses to the bars on the top of the beams, loads were placed on their ends (Fig. (1)), while were subjected to a process of accelerated corrosion throughout a period of about 5 months.

*Address correspondence to this author at the Engineering Department, Universidad Nacional del Sur, Bahía Blanca, Argentina;
E-mail: nfortega@criba.edu.ar

Table 1. Reinforcement Characteristics

	Diameter (mm)	Elastic Limit (MPa)	Ultimate Breaking Tensile Strength (MPa)
Longitudinal Reinforcement	4.2	680	690
Stirrups	2.1	302	414

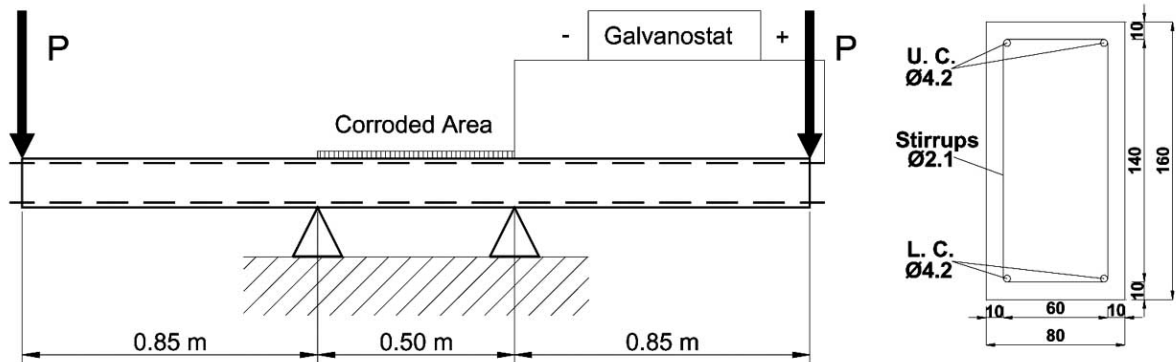


Fig. (1). Schematic model of essayed beams. a) Model of tested beams; b) Cross Section (units in mm).

In order to speed up corrosion, the central zone of the beams (0.50 m length) was kept permanently moistened with a solution of Sodium Chloride (Na Cl), 0.3 % by weight, to increase the medium's conductivity. The supports were placed on the edges of that area. Due to the adopted support conditions, an almost constant bending moment was ensured in the whole tested area (uniform stress on the rebars), being the beams subjected to self weight plus the action of different loads (SW + P), which varied from 0 to 1 kN. The flexural cracking load, for the geometric characteristics of the cross-section, structural model and employed materials, is approximately 0.8 kN.

A galvanostat provided a constant current intensity of 16.2 mA, in order to corrode an estimated rebar surface of 162 cm² (determined by the central zone of the top bars and part of the stirrups). In that way, an estimated current density of 100 µA/cm² was applied to the bars. Such an applied current density is about 10 times the measurement in highly corroded reinforced concrete structures [13], and it was also chosen in different papers about this subject [5, 14-16], be-

cause important attack penetrations in the bars could be obtained in convenient periods of time.

A counter-electrode was placed on the top of the beam, formed by a stainless steel mesh (50 cm length and as wide as the beam). A sponge was placed over the counter-electrode (same dimensions), which was kept permanently wet with the solution of Na Cl previously mentioned. In order to ensure that such wetting was constant, they were covered with an acrylic plate and then with nylon cover. A photograph obtained during the test can be seen in Fig. (2).

Cracks Measurement

The surface of the beams was daily observed from the beginning of the test, registering the appearance of the first stains and the first cracks. From that moment, the periodic measurement of their length and width was done with a graduated ruler, with a precision of 0.05 mm, in order to do a

Table 2. Concrete Composition and Characteristics

Component Materials (kN/m ³ of concrete):	
Common Portland Cement CPF40 IRAM 50000 [10]	3.00
Fine aggregate (natural siliceous sand)	8.64
Coarse aggregate (shingles MAS 25 mm)	10.50
Potable water (IRAM 1601* [11])	1.75
Water/Cement ratio	0.58
Average Fluidity (Abrams Cone) (cm)	8.0
Average Compressive Strength (MPa) (28 days)	23.9
Average Tensile Strength (MPa) (28 days)	2.37

(*IRAM 1601 establishes for reinforced concrete Cl⁻ ≤ 700 mg/dm³, SO²⁻ ≤ 1000 mg/dm³)



Fig. (2). Beams during the test.

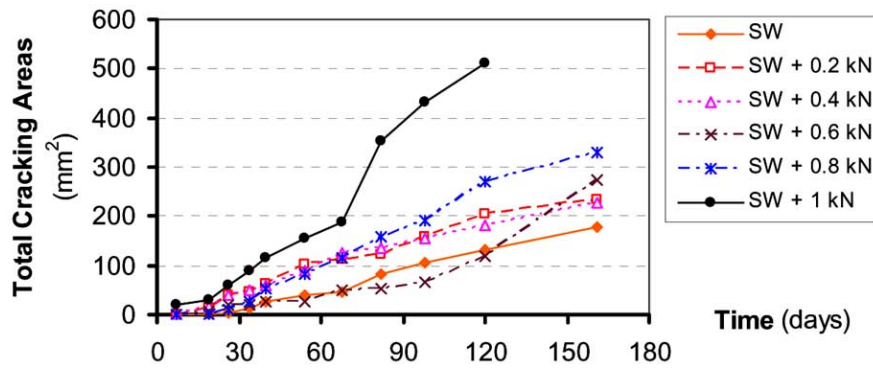


Fig. (3). Evolution of Total Cracking Areas vs. Time.

survey of the Cracking Areas (length x width) and of the Maximum Crack Widths reached.

Corrosion Potentials Determination

Simultaneously with the measurement of cracks, the survey of the Electrochemical Corrosion Potentials in different points of the beams over the upper bars was done. Corrosion Potentials were measured with current off, waiting an hour prior to measuring. This electrochemical parameter measures the activity of the corrosive process of the metallic bars embedded in the beams. For that reason, the information obtained from this non-destructive test is of real interest and is standardized by ASTM C 876-91 [17] and IRAM 1546 [18] standards.

The Corrosion Potentials were measured with a CANIN (PROCEQ) voltmeter, specially designed to analyze corrosion in concrete structures, employing a reference electrode of copper-copper sulphate (CCS).

RESULTS AND DISCUSSION

Cracking Areas

It is known that cracks known as “flexural cracks” are generated when stresses in the tensed areas of flexural reinforced concrete structures exceed the concrete’s tensile strength. They are identifiable by their transverse direction with regards to the main reinforcement bars. If the bars are also in a corrosive process, the corrosion products generate internal pressures because their volume is larger than the material from which they were originated. These pressures cause some products to fill the pores, others move to the ex-

terior through the flexural cracks (if any) and the rest generate stresses. When these stresses exceed the concrete’s tensile strength, cause lengthwise cracks to appear. These cracks will be known as “corrosion cracks”.

The aforementioned difference in crack direction allowed us to classify them in that way. But it is important to note that both types of cracks are linked by a close relationship. In fact, the presence of flexural cracks accelerates oxygen, water and chlorides’ penetration towards the rebars, favoring their corrosion process. On the other hand, since flexural cracks are exit ways for a part of the corrosion products, they could expand. Total growth of cracking causes the decrease of the load-bearing section of the beam (due to loss of the areas of steel and concrete) which could result in the structure’s collapse under heavy loads. This happened in our test, in the most heavily-loaded beam.

The survey of the Total Cracking Areas (Flexural Cracking Areas + Corrosion Cracking Areas) has been shown in Fig. (3), as a function of test Time. The behavior of the most loaded beam can be seen to be different from the others, due to the great influence of its flexural cracking.

It is shown that for each level of load, the Cracking Areas follow a behavior that could be fitted to a linear variation, with an adequate correlation, as can be seen in Table 3. It must be pointed that the determination of these equations was made in order to compare different gradients that determine process evolution rate.

It is evident that the progressive increase of the Total Cracking Areas throughout the test is directly related to the increase in rebar stress (represented by the beam’s load).

Table 3. Total Cracking Areas (At (mm²)) Variation Trend in Time (t (days))

Load	Name	Equation	Coefficient of Determination (R²)
SW (Self Weight)	B 16	$A_t = 1.258 t - 23.682$	0.984
SW+ 0.2 kN	B 13	$A_t = 1.602 t - 3.486$	0.977
SW+ 0.4 kN	B 14	$A_t = 1.524 t - 0.212$	0.977
SW+ 0.6 kN	B 12	$A_t = 1.502 t - 36.636$	0.833
SW+ 0.8 kN	B 11	$A_t = 2.380 t - 40.765$	0.986
SW+ 1.0 kN *	B 15	$A_t = 4.689 t - 61.802$	0.960

(*The test ended 30 days earlier, due to sample breakage).

With linear equations, the line's gradient could be interpreted as the cracking area variation (mm^2) in the unit of time (day). Observing the obtained linear equations, a clear increase of daily cracking can be seen, as the load on the beam increases; or more accurately, the more increase the bar stresses, the bigger become the cracks.

In a previous author's paper [5], the trend of Total Cracking Areas was obtained as a function of Time for beams in similar conditions and materials but supported in their full length (in such a way to avoid any possible stresses than those resulting from concrete shrinkage). In this case, the gradient was lower than those obtained in most of the beams under loads ($A_t = 1.164 t - 31.460$).

It can be said that in previous papers, with pre-stressed beams [6], the variation of Total Cracking Areas with respect to Time that best fitted tend to be quadratic, whereas in the current case, linear variation fits well enough. This difference could be originated by the compression over the concrete cover of the bars, being pre-stressed structures, tends to spall out more quickly.

Maximum Cracking Widths

Analyzing the behavior of the Maximum Cracking Widths as a function of test Time, they do not seem to clearly follow any certain laws. As can be seen in Fig. (4), times where maximum widths remain constant alternate with important increases. Trying to define a law that approximately describes the phenomenon we present linear variations which show a good approximation in most beams, in

Table 4. When interpreting the phenomenon with these trend lines, an increase in the gradients with the load increase can be seen in general. That is, the Maximum Cracking Widths grow daily and proportionately to the (increase in) tension stresses on the bars.

Appearance of the First Cracks

In the mentioned previous paper [5], with identical beams to the ones presented here but without bearing loads, the first corrosion cracks could be seen around the 40th day of the test. On the beams tested here, with stress on the rebars due to the acting loads, the earlier appearance of cracks was seen approximately on the 20th day, presenting all the beams corrosion cracks and some of them flexural cracks as well.

As previously mentioned, the flexural cracking load for the structural model and materials of the studied beams is 0.80 kN. Therefore, the appearance of cracks in the affected beams under lower loads should not be expected. In our case, almost all the beams showed some flexural cracks by the 40th day of the accelerated corrosion test (except the one subjected only to its own weight, which did not develop cracks during the whole test period). This gives an idea of the clear influence of corrosion over the cracking increase due to flexure.

Electrochemical Behavior

In [19], the analysis of the electrochemical behavior of beams similar to our own was made, but without any external loads over the bars. In it, three well-defined periods were

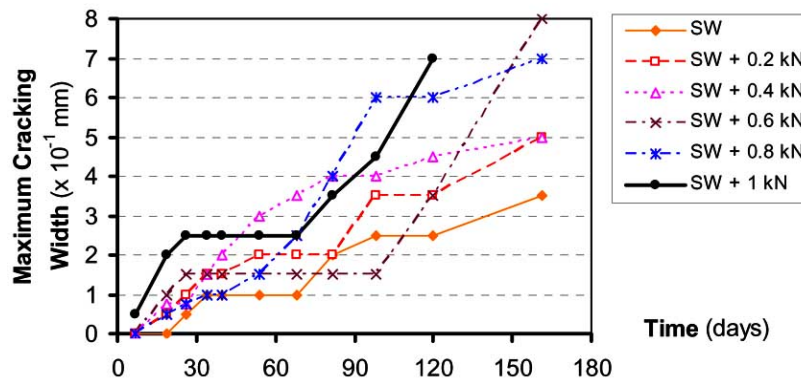


Fig. (4). Variation of Maximum Cracking Widths vs. Time.

Table 4. Maximum Cracking Widths ($W_{max}(\text{mm})$) Variation Trend in Time ($t(\text{days})$)

Load	Name	Equation	Coefficient of Determination (R^2)
SW (Self weight)	B 16	$W_{max} = 0.0023 t - 0.0122$	0.946
SW+ 0.2 kN	B 13	$W_{max} = 0.0024 t + 0.0387$	0.865
SW+ 0.4 kN	B 14	$W_{max} = 0.0034 t + 0.0441$	0.880
SW+ 0.6 kN	B 12	$W_{max} = 0.0038 t - 0.0355$	0.716
SW+ 0.8 kN	B 11	$W_{max} = 0.0025 t - 0.0619$	0.937
SW+ 1.0 kN *	B 15	$W_{max} = 0.0043 t + 0.0639$	0.831

(* The test ended 30 days earlier, due to sample breakage)

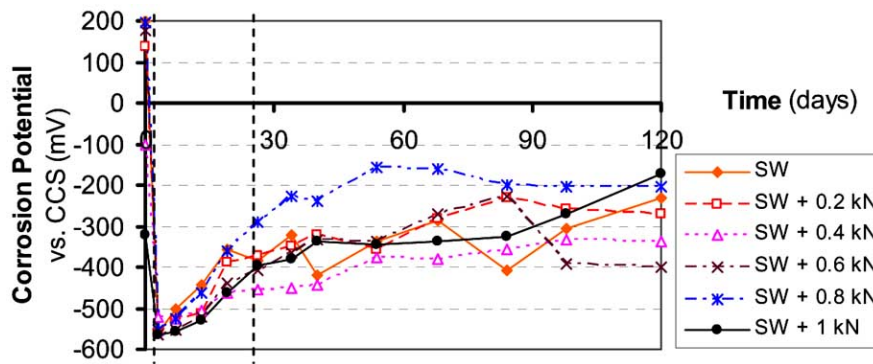


Fig. (5). Variation of Electrochemical Corrosion Potentials vs. Time.

Table 5. Comparison of Periods Between Loaded and Unloaded Beams

	Activation	Pseudo - Passivation	Corrosion Cracking
Unloaded beams	0 to 12 th day	12 th day to 42 nd day	42 nd day and beyond
Loaded beams	0 to 3 rd day	3 rd day to 26 th day *	26 th day and beyond

(*The beginning of cracking was detected on the 26th day in the beam subjected only to own weight; in most of the loaded beams it occurred earlier).

Table 6. Average Electrochemical Corrosion Potentials (E_{corr}) at the End of the Activation Period, and Towards the End of the Test

Load	Name	E_{corr} (Activation) (mV)	E_{corr} (End) (mV)
Self Weight (SW)	B 16	-560	-232
SW + 0.2 kN	B 13	-562	-269
SW + 0.4 kN	B 14	-556	-270
SW + 0.6 kN	B 12	-565	-399
SW + 0.8 kN	B 11	-552	-205
SW + 1.0 kN *	B 15	-566	-172

(*The test ended 30 days earlier, due to sample breakage).

found: *activation* (sudden potential decrease, towards very negative values), *pseudo-passivation* (potential increase, until the appearance of the first cracks) and *cracking* (minor potential increase, becoming general cracking). In the current case, where the reinforcements were under tension, the same three periods were found, but with clear differences in each duration. The variation of the Average Corrosion Potentials over Time can be seen in Fig. (5), showing the *activation*, *pseudo-passivation* and *cracking* periods.

A deep explanation of the Corrosion Potential variation in those three periods could be seen in the Appendix.

In Tables 5, the shortening of these periods in the loaded beams in comparison with those obtained in aforementioned Reference [19] (unloaded beams) is shown.

In Tables 6 the Average Electrochemical Corrosion Potentials are shown, with the values obtained for each beam during the third day (at the end of the activation period) and

on the 120th day of the test (before the failure of the most loaded beam).

At the end of the activation period (3rd column), no significant differences were appreciated in the Average Electrochemical Corrosion Potentials between the beams with different stress on their bars. However, a certain relationship between the stress increase in the bars and the Average Electrochemical Potentials could be distinguished when the cracking had generalized, towards the end of the test (4th column). As long as the flexural cracking load (SW + 0.8 kN) was not surpassed, more active potentials were obtained as the external load increased. This would indicate that the stress increase in the bars would delay passivation. But in the beams that exceeded the cracking load, the Average Electrochemical Corrosion Potentials became on less active values. The increased cracking provides a greater availability of oxygen to the rebars, increasing the formation of oxides and leading the bars to more passive potentials.

Table 7. Lengths (L) and Areas (Partial Area A, Total Area A_t) Effectively Affected by Corrosion in Each beam (on Stirrups, Upper Chords (U.C.) and Lower Chords (L.C.) of the Bars)

Loads (Name)	Corroded Element	L (mm)	A (mm ²)	A _t (mm ²)
Self Weight (SW) (B16)	Bars U.C.	1415		
	Bars L.C.	250	21969	33517
	Stirrups	1750	11545	
SW + 0.2 kN (B13)	Bars U.C.	1360		
	Bars L.C.	500	24542	37275
	Stirrups	1930	12733	
SW + 0.4 kN (B14)	Bars U.C.	1350		
	Bars L.C.	577	25426	36938
	Stirrups	1745	11512	
SW + 0.6 kN (B12)	Bars U.C.	1420		
	Bars L.C.	490	25202	39584
	Stirrups	2180	14382	
SW + 0.8 kN (B11)	Bars U.C.	1330		
	Bars L.C.	540	24806	38660
	Stirrups	2100	13854	
SW + 1.0 kN (B15) *	Bars U.C.	1400		
	Bars L.C.	1210	34570	51525
	Stirrups	2570	16995	

(*The test ended 30 days earlier, due to sample breakage).

Corrosion-Affected Area

On the unloaded beams presented in Reference [19], a point located 0.10 m outside the moistened area, reached similar Electrochemical Corrosion Potentials as the other ones located into this area, towards the end of the test (105th day). In the stressed beams of our test, this happened in a much shorter time (around 30th day) and from that point on, it had the same behavior as the other points inside the moistened zone. That is, the corrosion-affected area rapidly exceeded the anticipated corrosion area.

In order to find out the areas of the bars that were effectively affected by corrosion, the bars were uncovered and then surveyed.

The values of the affected areas resulting from the survey of the bars at the end of the test period (160 days) are shown in Table 7. In the most heavily-loaded beam (B15), the survey was done after the 130th day, immediately after it ruptured. It can be seen that corrosion extended beyond the upper chords (U.C.) and the upper part of the stirrups, even affecting the lower chords (L.C.). The length of corrosion in the reinforcements, initially assumed to be 1000 mm in the bars and 480 mm in the stirrups, were in fact almost double and quadruple those values respectively, in all the beams, becoming more evident in the most heavily-loaded beam.

Since the intended corrosion area was not confined, allowing corrosion to spread freely as in normal practice, the current density was not constant throughout the test. Only a constant current ($I = 16.2$ mA) was ensured by the gal-

vanostat. The actual affected area depends on the final length and diameter of the bars. The final length can be measured with a certain degree of precision. But it does not happen with the final diameter, due to the corrosion was not uniform (because of the pitting caused by the chlorides). For that reason, the actual affected area, in each step of the corrosive process, is very hard to determine.

As regards the relationship between applied load (rebar stress) and reinforcement corrosion extension, it is evident Table 7 that an increase in the affected areas exists both in bars and in stirrups between the beam loaded with just its own weight (B16) and the most heavily-loaded beam (B15) (even though the latter had a shorter testing time, due to its breakage). But it does not seem to be there a clear difference between beams affected with different stress conditions when the load is below the flexural cracking load (0.8 kN).

A gravimetric analysis was made in order to determine the loss of base material in the affected bars. In that way, the bars were cleaned of loose material by dipping them in a solution of chlorhydric acid as indicated in standard ASTM G1-67 [20]. No important gravimetric differences between the beams were found, despite the different loads and affected areas of the bars, as it was expected.

CONCLUSIONS

It was found in this research, that corrosion under stress of the rebars increased the structure's deterioration speed, which doubtlessly decreases the affected element's durabil-

ity. This was shown in the current experimental study, in the following aspects:

1). Through observation of cracking:

The loaded beams exhibited cracks that advanced more quickly than in unloaded beams. A clear increase of the cracking with the increased rebar stress was verified.

As a consequence of the previous point, when State I (cracking limit) was surpassed by flexure in the reinforced concrete, cracking was favored, increasing both types of cracks with great speed, even leading to the structure's collapse (which occurred in the most heavily-loaded beam in this test).

When concrete is free of stresses or just compressed, Cracking Areas as a function of Time follow a second degree parabola. In this case, where concrete is in tension, its variation followed a linear behavior.

When the load on the beams increased, the variation of the Maximum Cracking Widths presented a clear increase in time.

The first cracks appeared earlier in the loaded beams than in the unloaded ones. This fact, as well as the increase in Cracking Areas and Maximum Cracking Widths, reaffirms that stresses in the reinforcements speed up the effects of the corrosion.

2). Through the electrochemical process:

Through the survey of the Electrochemical Corrosion Potentials, an acceleration of the periods of activation, pseudo-passivation and cracking was found on the loaded beams, with regards to the unloaded ones.

The increase in rebar stress appeared to have influence in the delay of pseudo-passivation, as long as the flexural cracking load was not reached. When that limit was crossed, more passive potentials were obtained.

3). The area of reinforcements affected by corrosion quickly exceeded the initially assumed hypothesis. A direct relationship between the affected area and the acting stress in the bars was not found for loads below the flexural cracking load; however, once said load was surpassed, the corrosion extension was much larger, in the most heavily-loaded beams.

ACKNOWLEDGMENTS

This work was fully supported by the Bureau of Science and Technology of the Universidad Nacional del Sur, Bahía Blanca, Argentina.

The authors would like to thank the Laboratorio de Estudios y Ensayos de Materiales, the Laboratorio de Suelos, and Laboratorio de Modelos Estructurales' technician Juan Pablo Gorordo, of the Departamento de Ingeniería of the Universidad Nacional del Sur, for his help during the tests.

NOMENCLATURE

A	=	Partial Areas (on the affected bars)
A	=	Total Areas (on the affected bars)
B	=	Beam

CCS	=	Copper-Copper Sulphate (reference electrode)
E_{corr}	=	Electrochemical Corrosion Potential
L	=	Length
LC	=	Lower Chord (on reinforcement)
NaCl	=	Sodium Chloride
P	=	Applied load
R^2	=	Approximation Index
Rebars	=	Reinforcement bars
SW	=	Self Weight
T	=	Time
UC	=	Upper Chord (on reinforcement)
W_{max}	=	Maximum Cracking Width

SUPPLEMENTARY MATERIAL

Appendix File

This appendix contains a greater explanation of the electrochemical behavior of reinforced concrete beams without loads submitted to accelerated corrosion, Reference [19].

APPENDIX

Electrochemical Behaviour Obtained in Reinforced Concrete Beams Without External Load, Ref. [19]

A research of beams with different separation of stirrups but with similar material, longitudinal reinforcement, conditions of test and with the beams supported in all its length (to diminish tensions in the reinforcements), was made by this authors, in order to show the periods of different electrochemical behaviour (through the Corrosion Potentials). From the analysis of the Corrosion Potentials of the tested zone, it was concluded that all the beams had a behavior with equal tendency, during the studied period.

“It can be considered that the Corrosion Potentials vary according to 3 slopes, distinguishing according to them, three periods in the accelerated corrosion [19]:

- 1) From the beginning of application of the current to reaching the maximum negative potential. It is a very short period (2 to 12 days), where the slope of the curve of Potentials is important, and negative. It is an **activation process**, characterized by the modification of the passive state maintained by stabilized oxide in front to the cement alkalinity ($\text{pH} \geq 12$), due to the moistening with a solution of NaCl.
- 2) From the maximum negative potential, until the appearance of the first crack. This period includes between 30 and 40 days, and the slope of the curve becomes positive and minor enough, so that the potentials increase. It is a process of pseudo passivation, given by the consolidation of an oxide confined to the interphase, in contact with the concrete. Products of corrosion of greater volume are introduced within pores, saturating them. From this, they pressure the concrete, until crack it.
- 3) Since the appearance of the first crack, the behavior of each one of the points in the wetted zone is different; a

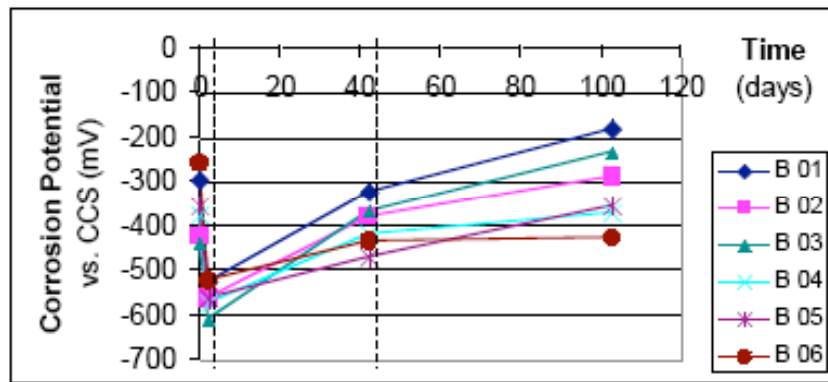


Fig. (6). Variation of the Corrosion Potentials Average vs. Time (beams with different separation of stirrups).

separation of slopes in each case is observed, which are smaller than the previous one. It can be seen in addition, that the points in which appeared the first cracks in each case, have in general a slope greater than not cracked ones. When concrete cracked, the way of oxygen is facilitated and tends to strengthen the pseudo passivation, taking to the present iron in oxides to a state of greater valence. This is the **cracking stage**, where a process of change of the quality of oxide (produced by the fast interchange with environment facilitated by the cracks) takes place”.

Fig. (6) shows the mentioned tendency obtained (in each beam) of the Corrosion Potentials Average in Time. The beams employed in the present work have equal distribution of stirrups to the beam B 01. From the comparison of the Fig. (5) and (6), it can be noted that the beginning of the last period (appearance of the first cracks) in Fig. (6) is overdue. This is due to the beams were unloaded.

REFERENCES

- [1] R.N. Swamy and S. Tanikawa, “An external surface coating to protect concrete and steel from aggressive environments”, *Materials and Structures*, vol. 26, pp. 465-78, 1993.
- [2] O. Cascudo and P. Helene, “Comportamiento mecánico del recubrimiento frente a los productos de corrosión de las armaduras”, *Hormigón y Acero*, vol. 214, pp.75-83, 1999.
- [3] M.C. Andrade, M.C. Alonso and F.J. Molina, “Cover cracking as a function of bar corrosion: part i – experimental test”, *Materials and Structures*, vol. 26, pp. 453-464, 1993.
- [4] J. Rodríguez, L.M. Ortega, J. Casal and J.M. Diez, “Estudio Experimental sobre la Capacidad Portante de Soportes de Hormigón con Armaduras Corroídas”, *Hormigón y Acero*, vol. 208, pp. 49-62, 1998.
- [5] R.R. Aveldaño, N.F. Ortega and L.N. Señas, “Influencia de la distribución de estribos en la fisuración en vigas de hormigón armado afectadas por corrosión de sus armaduras”, in *Proceedings of 14th Reunión de la Asociación Argentina de Tecnología del Hormigón, Argentina*, 2001, pp. 133-40.
- [6] N.F. Ortega, M.C. Alonso, M.C. Andrade and C. López, “Análisis de la fisuración ocasionada por la corrosión de las armaduras activas de elementos pretensados”, in *Proceedings of Coloquia 2001*, Madrid, 2001, pp. 10.
- [7] N.F. Ortega, C. López, M.C. Alonso and M.C. Andrade, “Mecánica estructural de elementos de hormigón, con armaduras activas adherentes sometidas a la corrosión”, in *Proceedings of 14th Reunión de AATH, Argentina*, 2001, pp. 99-106.
- [8] Instituto Argentino de Racionalización de Materiales IRAM 1546, *Portland Cement Concrete: Compression Test Method*, 1992.
- [9] American Society for Testing and Materials ASTM C496-71, *Standard Test Method for splitting tensile strength of cylindrical concrete specimens*, 1996.
- [10] Instituto Argentino de Racionalización de Materiales, IRAM 50000: *Cement. Common Cement. Composition, specifications, conformity evaluation and reception conditions*, 2000.
- [11] Instituto Argentino de Racionalización de Materiales, IRAM 1601: *Water for mortar and Portland cement concretes*, 1986.
- [12] Centro de Investigación de los Reglamentos Nacionales de Seguridad para las Obras Civiles del Sistema INTI, CIRSOC; “Reglamento Argentino de Estructuras de Hormigón”, *Buenos Aires*, vol. 1, p. 34, 2002.
- [13] J. Rodríguez, L.M. Ortega and A.M. García, “Medida de la velocidad de corrosión de las armaduras en estructuras de hormigón, mediante un equipo desarrollado dentro del proyecto eureka EU 401”, *Hormigón y Acero*, vol. 189, pp. 79-91, 1993.
- [14] C. Alonso, C. Andrade, J. Rodríguez and J.M. Diez, “Factors controlling cracking in concrete affected by reinforcement corrosion”, *Materials and Structures*, vol. 31, pp. 435-41, 1998.
- [15] J. Rodríguez, L.B. Ortega, J. Casal and J.M. Diez, “Comportamiento Estructural de Vigas de Hormigón con Armaduras Corroídas”, *Hormigón y Acero*, vol. 202, pp.113-31, 1996.
- [16] A. T. Acosta and A. Sagüés, “Concrete Cover Cracking and Corrosion Expansion of Embedded Reinforces Steel”, in *Proceedings of 3rd. NACE Latin American Corrosion Congress (LATINCORR 98)*, México, 1998, pp. 15.
- [17] American Society for Testing and Materials ASTM C 876-91, *Standard Test Method for Half Cell Potentials of Reinforcing Steel in Concrete*, 1991.
- [18] Instituto Argentino de Racionalización de Materiales IRAM 738, *Corrosión Electroquímica de Metales. Estructuras de Hormigón Armado y Pretensado. Método de medición de potenciales espontáneos de armadura de acero*, 1999.
- [19] R.R. Aveldaño, N.F. Ortega N.F. and J.B. Bessone, “Influencia de la Distribución de Estribos en los Potenciales de Corrosión en Vigas de Hormigón Armado”, in *Proceedings of Jornadas SAM-CONAMET-AAS 2001*, Argentina, p. 8, 2001.
- [20] American Society for Testing and Materials ASTM G1-67, *Recommended practice for preparing, cleaning and evaluating corrosion test specimens*, 1971.